Optimal Design of Energy Storage System for Peak-Shaving in Industrial Production

Lixin Li[1]*, Anna Sina Starosta[1], Bernhard Schwarz[1], Nina Munzke[1], Hanns-Martin Strehle[2], Mark Richter[2], Marc Hiller[1]

[1]Electrotechnical Institute, Karlsruhe Institute of Technology (KIT), Karlsruhe, Germany
[2]Fraunhofer Institute for Machine Tools and Forming Technology (IWU), Chemnitz, Germany
*lixin.li@kit.edu

Abstract

Energy storage systems (ESS) offer a wide range of applications in industrial production, with the potential to significantly reduce electricity power costs through peak-shaving, particularly in Germany. This paper proposes a methodology for designing ESSs specifically for industrial peak shaving from a techno-economic perspective. The proposed approach utilizes mixed-integer linear programming (MILP) to calculate the minimum annualized total operating costs, compares various energy storage technologies (EST) to determine the optimal solution, and performs sensitivity analysis to identify critical impact factors on the optimization problem. A case study is implemented with real-world data. The results indicate that connecting a 38.4 kW/38.4 kWh lithium-ion (Li-ion) battery energy storage system (BESS) to the example factory delivers the greatest economic benefit compared to the other three storage technologies. This results in a total cost saving of 980 €/a and a peak power reduction of 33.8 kW. Additionally, a lookup table is provided to assist the factory in selecting the optimal Li-ion BESS available in the market.

Keywords – energy storage technology, industrial production, mixed-integer linear programming, peak-shaving

1 Introduction

In recent years, there has been a growing interest in exploring the potential of energy storage systems (ESS) in the industrial sector. Various applications such as ancillary services, peak-shaving, and arbitrage have been actively investigated. Among these applications, peak-shaving has gathered significant attention due to its potential to reduce electricity power costs for factories while also contributing to network stability [1, 2]. The design process of ESS can be categorized into three main areas: energy storage technology (EST) selection, ESS sizing, and optimal operation of ESSs [1]. Each of these steps is crucial, and any improper design within these areas can result in increased costs and system losses.

Research efforts have been dedicated to addressing the complex optimization problem of designing ESS specifically for peak-shaving applications. Braeuer et al. [3] and Hong et al. [4] separately employed linear programming and heuristic algorithm to optimize the sizing of batteries for peak-shaving, yet they did not compare different ESTs. Similarly in [5], Lucas and Chondrogiannis focused on vanadium redox flow batteries (VRFB) for peak-shaving without providing a quantitative analysis of the reasoning behind their selection. On the other hand, Alsaidan et al. [6] studied different ESTs, aiming to minimize the microgrid operation costs but they did not consider peak-shaving costs in the objective function. Oudalov et al. [7] proposed an industrial ESS design method through dynamic optimization, but the optimal operation was determined with a known energy storage size. As highlighted above, previous studies have primarily focused on some specific aspects of the overall ESS design problem.

To address the existing gap in the literature, this paper presents an innovative design framework for optimal selecting, sizing, and operating an ESS specifically for the purpose of peak-shaving in industrial production. The key contributions of this article can be summarized as follows:

- A techno-economic ESS design methodology for peak-shaving in the manufacturing industry is proposed.
- A generalized ESS model applicable to different types of ESTs considering various system parameters is developed.

The remainder of this paper is organized as follows. The whole design framework is described in Section 2. Section 3 introduces a mixed-integer linear programming (MILP) based optimization model for ESS design. Section 4 presents a case study with real-world data. The evaluation including sensitivity analysis is provided in Section 5. This paper is concluded in Section 0.

2 Design framework

The overall objective of the proposed methodology is to achieve the optimal design of an ESS for discrete production systems from an economic perspective. Thereby the scope can be the whole factory, a particular part of the production system (e.g., milling shop floor) or a specific machine (e.g., forming press). The design framework in Figure 1 can be structured as a four-step process, starting with the creation of a database of ESTs, followed by optimal sizing and optimal operation for each technology, continued with the selection of the best technology by comparing the optimization results of various technologies and finally a sensitivity analysis of the optimization model. The whole

The authors acknowledge the financial support by the Federal Ministry for Economic Affairs and Climate Action of Germany in the project ESiP (project number 03EI6062B).

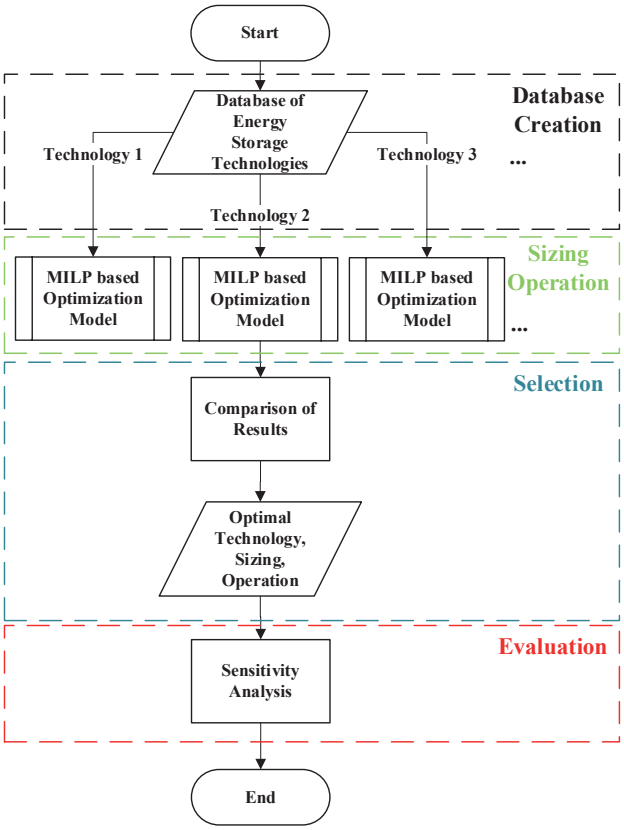

Figure 1 Flowchart of the design methodology of ESS.

process is based on a given electrical load profile of the production system or machine.

2.1 Database creation

The design solution for an ESS relies on two fundamental inputs: EST data and production data.

It is essential to have a comprehensive collection of core parameters for each EST. Different ESTs, such as various types of lithium-ion (Li-ion) batteries, VRFB, lead–acid (Pb-Acid) batteries, flywheels, and supercapacitors, exhibit distinct characteristics. A thorough comparison of ESTs is presented in previous works [8–12]. Table 1 presents a list of the essential parameters for all ESTs that will be utilized in the case study described in Section 4. It is important to note that all parameters considered in this study are taken from a system-level perspective.

The parameters listed in Table 1 are categorized into three groups. The first category contains economic parameters [12], which include energy related cost (consisting of battery capital cost, construction and commissioning cost) in €/kWh, power related cost (comprising the power conversion system and balance of plant) in €/kW, and operating and maintenance (O&M) cost in €/(kW-a). These three costs together form the total cost of an ESS. It is worth noting that flywheel energy storage (FES) is measured only in €/kW due to its low specific energy. The values provided in the table are based on the exchange rate of 0.95 between the US dollar and the euro in the previous year [13]. Price plays a crucial role in the process of selecting the appropriate EST, as only ESSs that offer economic benefits are considered viable for industrial production. Excessively high storage costs can make it economically unprofitable for industrial producers. However, it is important to note that price is not the sole determining factor. The second category comprises efficiency related parameters, such as system efficiency, depth of discharge (DoD), discharge time, and self-discharge. These parameters determine the actual energy and power that can be extracted from and delivered to an ESS. In terms of discharge time, the values for the three types of electrochemical ESTs are set at 1 h, while the flywheel has a faster discharge time of 0.25 h. Additionally, the flywheel exhibits a high self-discharge rate. The last classification concerns the degradation related parameters, which include cycle life and calendar life. Typically, the lifetime value is determined when the remaining energy capacity of batteries decreases from 100% to 80% [14].

Table 1 Parameters of ESTs [8–12]

Parameters	Units	Li-ion	VRFB	Pb-Acid	Fly-wheel
Costs					
Energy Related	€/kWh	353	707	414	–
Power Related	€/kW	368	427	427	1026
O&M	€/kW/a	9.5	9.5	9.5	5.3
Efficiencies					
Battery Cycle	%	95	70	80	90
Average Inverter	%	95	95	95	95
System	%	93	79	85	90
DoD	%	80	80	80	80
Discharge Time	h	1	1	1	0.25
Self-Discharge	%/h	0	0	0	20
Lifetimes					
Calendar	a	10	15	10	20
Cycle	–	3,000	10,000	2,000	200,000

The design process of an ESS necessitates a comprehensive analysis that encompasses not only the characteristics of the EST itself but also the specific production process. Therefore, an additional crucial dataset to consider is the production data, typically represented by the factory load profile. By examining basic load profile characteristics, such as the period, maximum power, and cycle total energy consumption, the initial screening of ESTs can be implemented. Furthermore, a detailed load profile can be employed for the precise sizing of the ESS.

2.2 Sizing and operation

The primary task of this step is to design ESSs and develop operation plans utilizing different ESTs for a given production process. To achieve this, the optimal sizing and oper-

ation problem is formulated as a MILP problem. The objective function aims to minimize the overall operating costs. Several constraints are imposed on the ESS, which are derived from the characteristics of the ESTs and other limitations associated with the utility grid. To find the optimal solution, a specialized software tool like MATLAB is employed. The difficulty of this part lies in balancing the conflict between the model complexity and the computation time. The Literature [15] suggests that reducing a nonlinear and complex ESS model to a linear model is a well-established approach. This simplification allows the optimization problem to be solved for an optimal solution. The detailed process of model building and solution finding will be explained in Section 3.

2.3 Comparison and selection

Optimization results will be obtained for each EST after solving the MILP problem, including optimal size, and optimal ESS operation strategy. Then the best EST will be selected in terms of economy and peak-shaving ratio. This step represents a subsequent optimization of the previous step (Subsection 2.2).

2.4 Evaluation

After the design is completed, sensitivity analysis [16, 17] is employed to determine how uncertainties in the input parameters affect the optimal design outcomes. To facilitate easy access to the optimization results without the need to rerun the optimization algorithm every time, a lookup table can be created. This table serves as a reference guide for plants and assists in making informed decisions regarding the selection of ESSs available in the market.

3 Model formulation

Figure 2 illustrates a simplified industrial distribution network with an ESS. In the absence of an ESS, the plant load is fully covered by the utility grid. However, with the integration of an ESS at a specific bus (AC-coupled), the system gains additional flexibility in controlling the power flow within each component, thus enabling the optimization of the overall system operation.

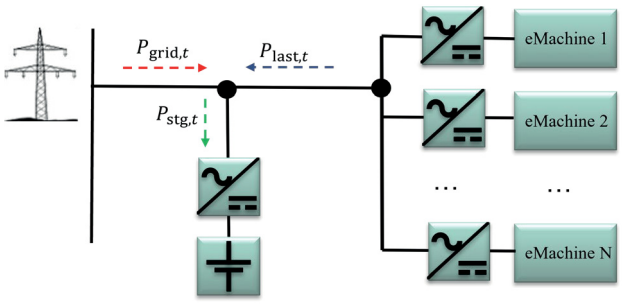

Figure 2 Schematic of an industrial distribution network with an ESS.

Various methods have been developed by numerous researchers to determine the size and power dispatch of ESSs [18]. In this paper, a single-objective optimization model based on MILP is proposed. To linearize the model, certain assumptions are made.

- The electric loss of the ESS is considered while the thermal loss and the loss of the management system are neglected.
- The system efficiency, including battery cycle efficiency and inverter efficiency, is set as a constant.
- All ESTs operate in their respective lifetime intervals without considering the degradation model.

3.1 Objective function

The objective of the optimization problem is to minimize the overall operating costs in Figure 2. Eq. (1), which derives from use case 2 in [3], shows that the objective function includes the annualized electricity power costs A_{peak}, the annualized system costs of ESS $A_{\text{ESS\_sys}}$ and the annualized maintenance costs of ESS $A_{\text{ESS\_O\&M}}$.

$$\min\left(A_{\text{peak}} + A_{\text{ESS\_sys}} + A_{\text{ESS\_O\&M}}\right) \tag{1}$$

A_{peak} is calculated in (2), where $\text{C}_{\text{grid\_power}}$, U_{peak} are the grid power cost and the peak demand. $A_{\text{ESS\_sys}}$ in (3) represents the annualized system costs, where $\text{C}_{\text{ESS\_cap}}$, $E_{\text{ESS}}^{\text{nom}}$, $\text{C}_{\text{ESS\_power}}$, $P_{\text{ESS}}^{\text{nom}}$, CRF are the ESS energy related cost, the nominal ESS capacity, the ESS power related cost, the nominal ESS power, and the capital recovery factor, respectively. $A_{\text{ESS\_O\&M}}$ is calculated by multiplying the O&M cost $\text{C}_{\text{ESS\_O\&M}}$ and $P_{\text{ESS}}^{\text{nom}}$.

$$A_{\text{peak}} = \text{C}_{\text{grid\_power}} \cdot U_{\text{peak}} \tag{2}$$

$$A_{\text{ESS\_sys}} = \left(\text{C}_{\text{ESS\_cap}} \cdot E_{\text{ESS}}^{\text{nom}} + \text{C}_{\text{ESS\_power}} \cdot P_{\text{ESS}}^{\text{nom}}\right) \cdot \text{CRF} \tag{3}$$

$$A_{\text{ESS\_O\&M}} = \text{C}_{\text{ESS\_O\&M}} \cdot P_{\text{ESS}}^{\text{nom}} \tag{4}$$

CRF allows costs to be calculated on an annualized basis, taking into account the useful life of the entire system and interest rates [19],

$$\text{CRF} = \left(I \cdot (1+I)^T\right) / \left((1+I)^T - 1\right)\ [-/\text{a}] \tag{5}$$

where I and T are the interest rate and the lifetime of the ESS, respectively. I is set to be 2% [20].

3.2 Constraints

Distribution network system level constraints include nodal power balance and utility grid power limitation. The nodal power balance (6) ensures that the load demand P_{load} is always met by the utility grid power P_{grid} and the ESS power P_{ESS}, where P_{ESS} is positive when charging ($P_{\text{ESS\_chg}} > 0$, $P_{\text{ESS\_dhg}} = 0$) and negative when discharging ($P_{\text{ESS\_chg}} = 0$, $P_{\text{ESS\_dhg}} > 0$). Constraints with $\forall t \in \mathbb{T}$ indicate that the condition should be satisfied at all times $\mathbb{T}$.

$$P_{\text{grid},t} + P_{\text{load},t} = P_{\text{ESS},t} \quad \forall t \in \mathbb{T} \tag{6}$$

$$P_{\text{ESS},t} = P_{\text{ESS\_chg},t} - P_{\text{ESS\_dhg},t} \quad \forall t \in \mathbb{T} \tag{7}$$

Eq. (8) – (9) impose a maximum power from the grid, i.e., the threshold of peak-shaving U_{peak}. And this threshold is less than the maximum value of the load curve $\text{P}_{\text{load}}^{\text{max}}$.

$$P_{\text{gird},t} \leq U_{\text{peak}} \quad \forall t \in \mathbb{T} \tag{8}$$

$$U_{\text{peak}} \leq \mathrm{P}_{\text{load}}^{\max} \tag{9}$$

ESS level constraints include power, state of charge (SoC) and charge/discharge capacity. Inequality constraints (10) limit the charge and discharge power of the ESS to the $P_{\text{ESS}}^{\text{nom}}$, where η_{ESS} is the efficiency of the ESS, consisting of the inverter efficiency η_{cvt} and the storage efficiency η_{stg}.

$$\begin{aligned} &P_{\text{ESS\_chg},t} \cdot \eta_{\text{ESS}} \leq P_{\text{ESS}}^{\text{nom}} \ \ \forall t \in \mathbb{T} \\ &P_{\text{ESS\_dhg},t} / \eta_{\text{ESS}} \leq P_{\text{ESS}}^{\text{nom}} \ \ \forall t \in \mathbb{T} \\ &\eta_{\text{ESS}} = \eta_{\text{cvt}} \cdot \sqrt{\eta_{\text{stg}}} \end{aligned} \tag{10}$$

The working mode of the ESS is limited by (11), where $flg_{\text{ESS\_chg}}$ and $flg_{\text{ESS\_dhg}}$ are integer variables. With this constraint, the ESS can only be in charging ($flg_{\text{ESS\_chg}}$ = 1), discharging ($flg_{\text{ESS\_dhg}}$ = 1) and standby ($flg_{\text{ESS\_chg}}$ = $flg_{\text{ESS\_dhg}}$ = 0) states.

$$\begin{aligned} &P_{\text{ESS\_chg},t} \leq flg_{\text{ESS\_chg},t} \cdot \mathrm{P}_{\text{load}}^{\max} \ \ \forall t \in \mathbb{T} \\ &P_{\text{ESS\_dhg},t} \leq flg_{\text{ESS\_dhg},t} \cdot \mathrm{P}_{\text{load}}^{\max} \ \ \forall t \in \mathbb{T} \\ &flg_{\text{ESS\_chg},t} + flg_{\text{ESS\_dhg},t} \leq 1 \ \ \forall t \in \mathbb{T} \end{aligned} \tag{11}$$

Eq. (12) represents the conversion of power to energy, where L_{sd} and T_{step} are the self-discharge rate of ESS and time step, respectively.

$$\begin{aligned} E_{\text{ESS},t+1} = E_{\text{ESS},t} + T_{\text{step}} \cdot (P_{\text{ESS},t} - L_{\text{sd}} \\ \cdot E_{\text{ESS},t}) \ \ \forall t \in \mathbb{T} \end{aligned} \tag{12}$$

The energy content of the ESS is limited by setting the upper limit $\mathrm{SoC}_{\text{ESS}}^{\max}$ and the lower limit $\mathrm{SoC}_{\text{ESS}}^{\min}$.

$$\begin{aligned} \mathrm{SoC}_{\text{ESS}}^{\min} \cdot E_{\text{ESS}}^{\text{nom}} \leq E_{\text{ESS},t} \leq \mathrm{SoC}_{\text{ESS}}^{\max} \cdot E_{\text{ESS}}^{\text{nom}} \\ \forall t \in \mathbb{T} \end{aligned} \tag{13}$$

Eq. (14) limits the charge/discharge capacity of the storage by using the charge/discharge time τ_{ESS} in Table 1.

$$P_{\text{ESS}}^{\text{nom}} \cdot \tau_{\text{ESS}} = E_{\text{ESS}}^{\text{nom}} \tag{14}$$

To summarize, (1) – (5) and (6) – (14) describe the objective function and constraints of the optimization problem, respectively.

4 Case study

This section presents a case study based on real collected data. The first three steps of the four-step design process proposed in Section 2 will be applied in this section, and the last step will be proposed in Section 5.

4.1 Database creation

In the case study, a real electrical load profile from a medium-sized factory in the field of tool and die making with 100 employees is used (automotive supplier). It was measured at the central grid connecting point of the factory. The main consumers in the factory are the forming presses, milling machines, welding equipment and compressed air systems. Table 2 shows some key values of the load curve. The one-year load curve was divided into production weeks. To reduce the size of the variables and the calculation time, one characteristic week was selected. In the next steps of sizing, this week was simply repeated throughout the year (52 times). With this first approach, the uncertainties in the load profile through fluctuations in production utilization and seasonal consumption were neglected. A duration factor is calculated by dividing annualized electrical energy by maximum electrical power. According to the latest price list [21] of the German grid operator named Netz-BW, the power price is set to be 131 €/kW.

Table 1 Basic Information Load Profile

Features	Units	Values
Cycle Length	week	1
Annualized Electrical Energy	MWh	2,128
Maximum Electrical Power	kW	482
Duration Factor	h/a	7,492
Electrical Power Price	€/kW	131

The sampling resolution of the load profile is 15 minutes, which means that there are 4 · 24 · 7 = 672 sampling points in a period of one week, i.e., in this case T_{step} = 0.25 h and $\mathbb{T}$ is shown in (15).

$$\mathbb{T} = \{1, 2, 3 \cdots 672\} \tag{15}$$

The bottom limit of the curve is about 110 kW, indicating that this value is the base load of the factory, while the peak load is about 482 kW, which is more than four times the base load. It can be inferred that it is possible to reduce the overall costs through peak-shaving with an ESS. The databank of ESTs has been introduced in Subsection 2.1. For the purpose of this case study, four specific technologies have been selected as examples to individually optimize their sizing and operation. These technologies include Li-ion batteries, Pb-Acid batteries, VRFB, and flywheels.

4.2 Sizing and operation

Building upon the optimization model described in Section 3, the second step of the methodology is carried out. This model is implemented and solved using the optimization toolbox available in MATLAB. The MILP-based optimization model offers the advantage of finding the optimal solution. The resulting optimization outcomes are presented in Figure 3 and Table 3.

Each column in Figure 3 represents an optimized operation design for one EST. In each column, the top graphic shows the threshold of peak-shaving (U_{peak}), the power flows of the load (P_{load}) and the utility grid (P_{grid}). Sharp peaks in the load that exceed the threshold are covered by the power provided by the storage, whose power curve (P_{ESS}) and SoC are presented in the bottom graphic. The first column about the Li-ion BESS, is taken as an example. The calculated optimal threshold is 448.2 kW, which means that all the load between 448.2 kW and 482 kW can be covered by the Li-ion BESS during the production cycle, and 38.4 kWh of capacity is required for this purpose.

From the first three columns, it is clear that the three electrochemical ESSs perform similarly in terms of peak clipping effects. Their respective optimal designs can cover peak power over about 450 kW. They successfully address four peaks in the load curve through 1-2 charge/discharge

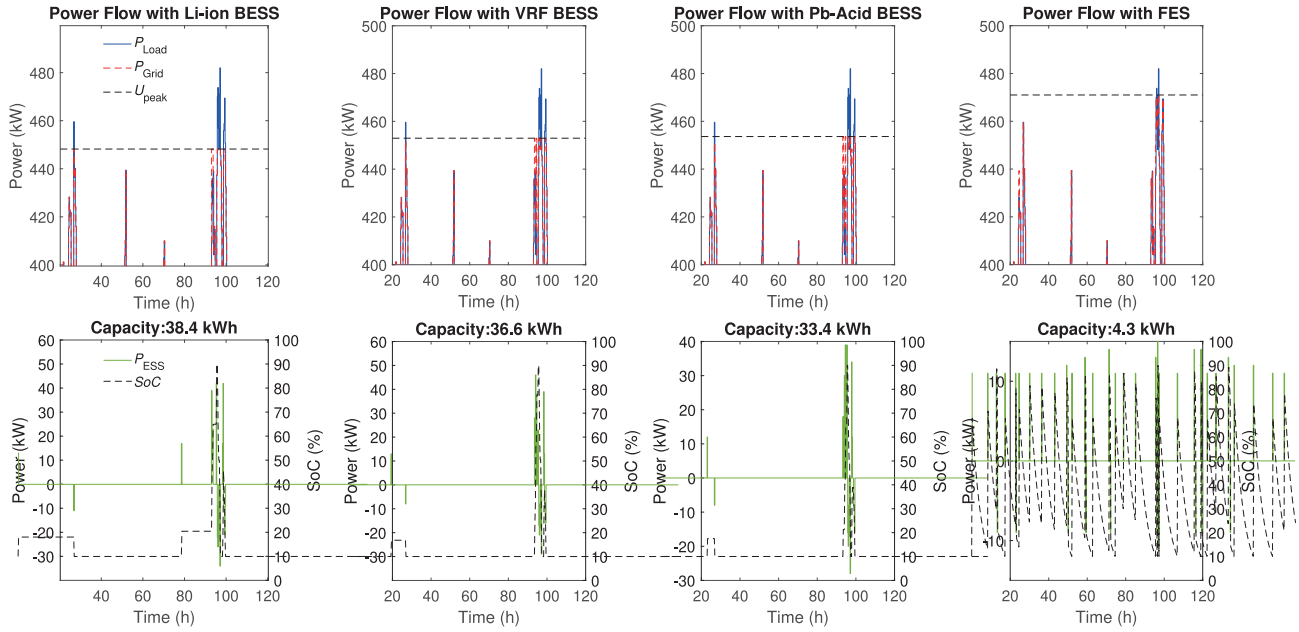

Figure 3 Comparison of peak-shaving of four different kinds of ESSs. Peak-Shaving occurs exclusively between 20 h and 120 h, so graphics are zoomed in within this specific time range.

Table 3 Cost Comparison of Different Optimized ESSs

Parameters	Units	Li-ion BESS	VRF BESS	Pb-Acid BESS	FES
Threshold Peak-Shaving	kW	448.2	452.9	453.6	471
Ratio Peak-Shaving	%	7	6	5.9	2.3
System Loss	kWh/a	7.8	19.4	12.7	65.2
Power Cost	k€/a	58.7	59.3	59.4	61.7
ESS Cost	k€/a	3.1	3.2	3.1	1.1
Maintenance Cost	k€/a	0.36	0.35	0.32	0.09
Sum Costs	k€/a	62.16	62.85	62.82	62.89

cycles, with one peak occurring between 25 h to 30 h and three other peaks within the range of 90 h to 100 h. However, the performance of FES differs significantly. Due to the contradiction between the minimum SoC (set at 10%) and the high self-discharge rate (20%), the FES is always in cycles of charge and self-discharge. The optimized flywheel design can only cover two peaks above 471 kW, within the interval of 96 h to 98 h.

4.3 Comparison and selection

For comparison purposes, the optimization results of the four ESTs are summarized in Table 3. Li-ion BESS (ST1) helps the plant to achieve the most economical operation, not only cutting 7% of the peak load in the production curve but also saving about 980 €/a. It is interesting to note that despite the many differences between VRF BESS (ST2) and Pb-Acid BESS (ST3) in terms of price, efficiency, lifetime and other parameters, their respective optimal designs achieve almost the same result, with a 6% peak-shaving rate at an annualized cost of about €62.9k. At the same time, they both perform worse than ST1. Additionally, FES is the worst choice of them all, and it achieves only a 2.3% peak-shaving rate for almost the same cost as ST2 and ST3. A major reason for this is its overly expensive price.

$$\Delta = (A_{\mathrm{ESS\_sys}} + A_{\mathrm{ESS\_O\&M}}) \,/\, U_{\mathrm{peak}} \qquad (16)$$

To incorporate both economic considerations and the effect of peak-shaving, the investment per unit of peak-shaving power for each ESS is calculated using (16). The resulting order, from lowest to highest, is as follows: ST1 (102 €/kW) < FES (106 €/kW) < ST3 (121 €/kW) < ST2 (123 €/kW). The analysis reveals that the FES demonstrates a favorable price-to-performance ratio in this particular context. This indicates that flywheels with high power-to-energy ratios and high unit prices are most suitable for extreme power situations, i.e., extreme spikes with very high power and very little energy.

In addition, the system losses of ESSs are an important evaluation factor. The losses of ST1, ST2 and ST3 increase with decreasing cycling efficiency, whereas the system losses of FES are mainly derived from its high self-discharge rate.

In summary, the Li-ion battery is the best of the three electrochemical ESTs in terms of price, peak-shaving effect and system losses, while the FES is not the most suitable to be put into this factory because of its high price and high system losses. However, flywheel has a great potential for application in dealing with certain very high-power situations, which re mains to be studied. For this tool manufacturing plant (defined load profile), the optimal design is a 38.4 kW/38.4 kWh Li-ion BESS, and the optimal operating scheme is shown in the first column of Figure 3.

5 Evaluation

From the Subsections 4.2 and 4.3, it can be concluded that the ESS designed for this plant will only be used roughly 3-4 times during the production cycle of a week. However, this still makes sense from an economic point of view, as high electricity power costs can be reduced. The results show that the investment in the Li-ion BESS can get a total savings of 980 €/a. As the price of ESSs drops year by year, the benefits will become greater and greater. A similar conclusion is reached in [15]. The authors design an ESS for a profile and obtain the numbers of capped peaks of 20 with yearly billing scheme, and the full equivalent cycles of the ESS are only 5. But that BESS still brings benefits.

5.1 Sensitivity analysis

The data presented in Table 1 is sourced from [8–12], and discrepancies exist among the data obtained from these sources. Furthermore, certain parameters, such as energy and power related cost, exhibit variations over time. Thus, conducting a sensitivity analysis becomes crucial in assessing the influence of alterations in input parameters on the model's output results.

For the analysis, four parameters from Table 1 have been chosen: energy related cost, power related cost, discharge time, and calendar lifetime. The values listed in the table serve as the reference values. When altering one parameter, the remaining parameters are held constant at their respective reference values. This approach, known as the "one-at-a-time" approach [16], ensures that changes in a single parameter can be isolated and evaluated independently.

The results of the analysis conducted for Li-ion BESS are depicted in Figure 4. All the data presented in the figure have been normalized, where the reference case corresponds to the point (1, 1). The corresponding input parameters for the reference case can be found in the first column of Table 1, while the optimal sum costs associated with it are listed in the first column of Table 3. Figure 4 reveals that only the calendar lifetime exhibits a negative correlation with the annualized sum costs, and this correlation holds significance. On the other hand, the other three parameters demonstrate a positive correlation. Both energy related cost and power related cost display a relatively substantial impact on the annualized sum costs, with discharge time following closely. Based on the sensitivity analysis conducted on the Li-ion BESS, it can be concluded that the crucial parameters influencing the optimization results are the two related costs and the calendar lifetime. In other words, lower costs and an extended battery lifetime contribute to smaller annualized total operating costs of the plant. The same analytical procedure can be applied to the other ESSs to obtain comparable results.

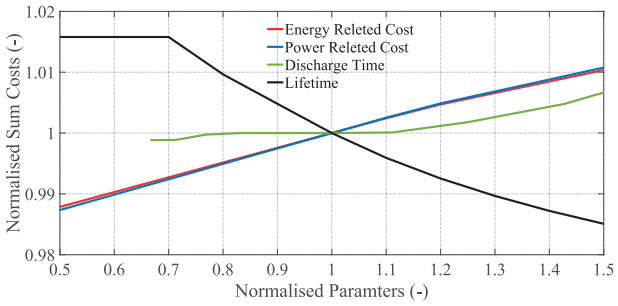

Figure 4 Impact of Li-ion BESS's parameters on annualized costs.

5.2 Lookup table

For the plant in the case study in Section 4, it is very practical to get a lookup table for a certain kind of EST. The plant can query the table for the respective optimal system design results under dynamic parameters. In this section, the energy related cost and power related cost are combined into one parameter, i.e., system cost. Then a one-dimensional lookup table for the optimal design of the Li-ion BESS with the parameter of the system cost is created. Table 4 shows that as the system cost increments from half the reference to 1.5 times the reference, the optimal ESS size decreases, the total cost increases (consistent with the analysis in the Subsection 5.1), and the peak-shaving ratio decreases. As the system cost decreases to half the reference price, the optimal ESS size increases to 56.3 kW/56.3 kWh while the peak-shaving ratio increases by 20%, which is a significant improvement. Figure 5 shows the power flow of the system under this design, where load demands higher than 441.2 kW are covered by the Li-ion BESS, and the 56.3 kWh capacity achieves a peak-shaving ratio of about 8.5%. On the other hand, when the system cost rises to 1.4 times the reference, Li-ion BESS will not be built at that plant because it will not be economically beneficial. In [12], the authors predict that the price of Li-ion BESS will reach down to 561 €/kW/kWh in 2025, with a decline of 22%. As the cost continues to drop, its potential for industrial peak shaving will continue to be explored.

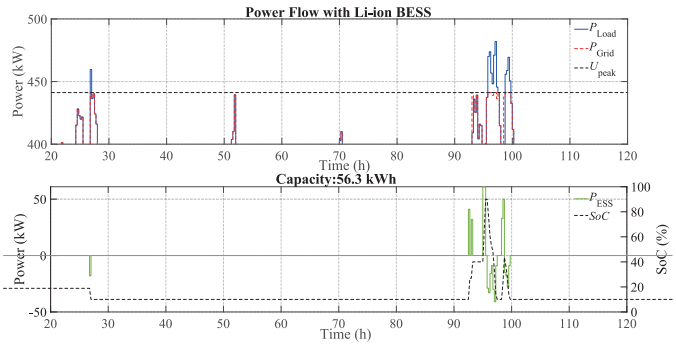

Figure 5 Power flow of Li-ion BESS with half of the reference system cost.

Table 4 Lookup Table for Optimal Li-ion BESS Design

System Cost (baseline: 721 €/kW/a)	**Optimal Size** (−kW/−kWh)	**Sum Costs** (baseline: 62.16 k€/a)	**Ratio of Peak-Shaving** (baseline: 7%)
0.5	56.3/56.3	0.97	1.2
0.6	38.4/38.4	0.98	1
0.8	38.4/38.4	0.99	1
1.0	38.4/38.4	1	1
1.2	29.8/29.8	1	0.81
1.4	–	1.02	0
1.5	–	1.02	0

6 Conclusion

A comprehensive ESS design methodology for peak-shaving in industrial production was proposed in this paper. The technology, size and operation of ESS were optimized. Moreover, a case study was performed. A 38.4 kW/38.4 kWh Li-ion BESS was designed for a medium-sized factory in the field of tool making. The follow-on work of this research will focus on building an ESS model considering heat losses and standby losses. A robust optimization approach that covers the uncertainty of the load profile must also be developed.

7 References

[1] M. Uddin, M. F. Romlie, M. F. Abdullah, S. Abd Halim, A. H. Abu Bakar, and T. Chia Kwang, "A review on peak load shaving strategies," *Renewable and Sustainable Energy Reviews*, vol. 82, pp. 3323–3332, 2018, doi: 10.1016/j.rser.2017.10.056.

[2] A. J. Pimm, T. T. Cockerill, and P. G. Taylor, "The potential for peak shaving on low voltage distribution networks using electricity storage," *Journal of Energy Storage*, vol. 16, pp. 231–242, 2018, doi: 10.1016/j.est.2018.02.002.

[3] F. Braeuer, J. Rominger, R. McKenna, and W. Fichtner, "Battery storage systems: An economic model-based analysis of parallel revenue streams and general implications for industry," *Applied Energy*, vol. 239, pp. 1424–1440, 2019, doi: 10.1016/j.apenergy.2019.01.050.

[4] Z. Hong, Z. Wei, J. Li, and X. Han, "A novel capacity demand analysis method of energy storage system for peak shaving based on data-driven," *Journal of Energy Storage*, vol. 39, p. 102617, 2021, doi: 10.1016/j.est.2021.102617.

[5] A. Lucas and S. Chondrogiannis, "Smart grid energy storage controller for frequency regulation and peak shaving, using a vanadium redox flow battery," *International Journal of Electrical Power & Energy Systems*, vol. 80, pp. 26–36, 2016, doi: 10.1016/j.ijepes.2016.01.025.

[6] I. Alsaidan, A. Khodaei, and W. Gao, "A Comprehensive Battery Energy Storage Optimal Sizing Model for Microgrid Applications," *IEEE Trans. Power Syst.*, vol. 33, no. 4, pp. 3968–3980, 2018, doi: 10.1109/TPWRS.2017.2769639.

[7] O. Alexandre, C. Rachid, and B. Antoine, "Sizing and optimal operation of battery energy storage system system for peak shaving application," 2007. [Online]. Available: http://ieeexplore.ieee.org/servlet/opac?punumber=4534843

[8] B. Zakeri and S. Syri, "Electrical energy storage systems: A comparative life cycle cost analysis," *Renewable and Sustainable Energy Reviews*, vol. 42, pp. 569–596, 2015, doi: 10.1016/j.rser.2014.10.011.

[9] B. Lian, A. Sims, D. Yu, C. Wang, and R. W. Dunn, "Optimizing LiFePO4 Battery Energy Storage Systems for Frequency Response in the UK System," *IEEE Trans. Sustain. Energy*, vol. 8, no. 1, pp. 385–394, 2017, doi: 10.1109/TSTE.2016.2600274.

[10] A. A. Kebede, T. Kalogiannis, J. van Mierlo, and M. Berecibar, "A comprehensive review of stationary energy storage devices for large scale renewable energy sources grid integration," *Renewable and Sustainable Energy Reviews*, vol. 159, p. 112213, 2022, doi: 10.1016/j.rser.2022.112213.

[11] E. Hossain, H. Faruque, M. Sunny, N. Mohammad, and N. Nawar, "A Comprehensive Review on Energy Storage Systems: Types, Comparison, Current Scenario, Applications, Barriers, and Potential Solutions, Policies, and Future Prospects," *Energies*, vol. 13, no. 14, p. 3651, 2020, doi: 10.3390/en13143651.

[12] K. Mongird *et al.,* "Energy Storage Technology and Cost Characterization Report," Pacific Northwest National Lab. (PNNL), Richland, WA (United States) PNNL-28866, 2019. [Online]. Available: https://www.osti.gov/biblio/1573487

[13] E. C. Bank, *ECB euro reference exchange rate: US dollar (USD).* [Online]. Available: https://www.ecb.europa.eu/stats/policy_and_exchange_rates/euro_reference_exchange_rates/html/eurofxref-graph-usd.en.html (accessed: Jul. 6 2023).

[14] N. Li, F. Gao, T. Hao, Z. Ma, and C. Zhang, "SOH Balancing Control Method for the MMC Battery Energy Storage System," *IEEE Trans. Ind. Electron.*, vol. 65, no. 8, pp. 6581–6591, 2018, doi: 10.1109/TIE.2017.2733462.

[15] R. Martins, H. Hesse, J. Jungbauer, T. Vorbuchner, and P. Musilek, "Optimal Component Sizing for Peak Shaving in Battery Energy Storage System for Industrial Applications," *Energies*, vol. 11, no. 8, p. 2048, 2018, doi: 10.3390/en11082048.

[16] D. M. Hamby, "A review of techniques for parameter sensitivity analysis of environmental models," *Environmental monitoring and assessment*, vol. 32, no. 2, pp. 135–154, 1994, doi: 10.1007/BF00547132.

[17] S. Negarestani, M. Fotuhi-Firuzabad, M. Rastegar, and A. Rajabi-Ghahnavieh, "Optimal Sizing of Storage System in a Fast Charging Station for Plug-in Hybrid Electric Vehicles," *IEEE Trans. Transp. Electrific.*, vol. 2, no. 4, pp. 443–453, 2016, doi: 10.1109/TTE.2016.2559165.

[18] M. A. Hannan, M. Faisal, P. Jern Ker, R. A. Begum, Z. Y. Dong, and C. Zhang, "Review of optimal methods and algorithms for sizing energy storage systems to achieve decarbonization in microgrid applications," *Renewable and Sustainable Energy Reviews*, vol. 131, p. 110022, 2020, doi: 10.1016/j.rser.2020.110022.

[19] V. I. Herrera, H. Gaztanaga, A. Milo, A. Saez-de-Ibarra, I. Etxeberria-Otadui, and T. Nieva, "Optimal Energy Management and Sizing of a Battery--Supercapacitor-Based Light Rail Vehicle With a Multiobjective Approach," *IEEE Trans. on Ind. Applicat.*, vol. 52, no. 4, pp. 3367–3377, 2016, doi: 10.1109/TIA.2016.2555790.

[20] "Long-term interest rate statistics for EU Member States," 2023. [Online]. Available: https://www.ecb.europa.eu/stats/financial_markets_and_interest_rates/long_term_interest_rates/html/index.en.html

[21] Netze BW GmbH, *Veröffentlichungen - Netze BW GmbH.* [Online]. Available: https://www.netze-bw.de/unternehmen/veroeffentlichungen#3-1-1 (accessed: Jul. 11 2023).